Impact of assimilated and interactive aerosol on Tropical Cyclogenesis.

O. Reale,[1,2] K. M. Lau,[1] A. da Silva,[3] T. Matsui,[1,4]

Corresponding author: O. Reale, NASA Goddard Space Flight Center, Code 610-AT, Greenbelt, MD 20771, USA. (oreste.reale-1@nasa.gov)

[1]Earth Science Division - Atmospheres, NASA Goddard Space Flight Center, Greenbelt, Maryland, USA.

[2]Goddard Earth Sciences Technology and Research, Universities Space Research Association, Columbia, Maryland, USA.

[3]Global Modeling and Assimilation Office, NASA Goddard Space Flight Center, Maryland, USA.

[4]Earth System Science Interdisciplinary Center, University of Maryland,College Park, Maryland, USA.

This article investigates the impact of Saharan dust on the development of tropical cyclones in the Atlantic. A global data assimilation and forecast system, the NASA GEOS-5, is used to assimilate all satellite and conventional data sets used operationally for numerical weather prediction. In addition, this new GEOS-5 version includes assimilation of aerosol optical depth from the Moderate Resolution Imaging Spectroradiometer (MODIS). The analysis so obtained comprises atmospheric quantities and a realistic 3-d aerosol and cloud distribution, consistent with the meteorology and validated against Cloud-Aerosol Lidar and Infrared Pathfinder Satellite Observation (CALIPSO) and CloudSat data. These improved analyses are used to initialize GEOS-5 forecasts, explicitly accounting for aerosol direct radiative effects and their impact on the atmospheric dynamics. Parallel simulations with/without aerosol radiative effects show that effects of dust on static stability increase with time, becoming highly significant after day 5 and producing an environment less favorable to tropical cyclogenesis.

1. Introduction

The possibility that the Saharan Air Layer (SAL) exerts some control on weather systems over the tropical Atlantic has been contemplated since the early '70s [e.g., Carlson and Prospero, 1972]. Among various studies, Karyampudi and Pierce [2002] conjectured that the SAL effect on the development of waves into tropical cyclones (TCs) could be modulated by seasonal precipitation over the Sahel, with a negative (i.e., suppressing) impact occurring only in dry seasons. Dunion and Velden [2003] attributed to the SAL a generally unfavorable role on tropical cyclogenesis, finding supported by a number of other studies [e.g., Sun et al. 2009]. On the other hand, Braun [2011] presents an overall critical view of the SAL as a TC-suppressing agent and suggests, among other concerns, the possibility that it may be dry air of non-Saharan origin that actually plays an inhibiting role, attributed erroneously to the SAL.

An important contribution to this ongoing debate stems from the ability of realistically simulating the aerosol radiative effects on the tropical atmosphere. The forerunner study [Tompkins at al., 2005] demonstrated the improvement caused by insertion of climatologically-varying aerosols in a global modeling setting. Since then, progress has been made to simulate increasingly realistic aerosols. Among several studies, Reale et al. [2011, hereafter RLD11] have shown that simulated aerosols, realistically varying with the meteorology and interacting with the atmospheric dynamics (instead of being climatologically prescribed), further improve the representation of the African Easterly Jet (AEJ).

A further step is represented by the ability to *objectively* define the SAL through a 3-dimensional dust distribution constrained by assimilated observed aerosols: i.e., to create a SAL analysis as a product of a DAS (Data Assimilation System). Until now, statements on the SAL borders have been limited by qualitative interpretation of satellite imagery and a categorical SAL definition based on a subjectively chosen threshold of aerosol optical depth (AOD). A degree of subjectivity is also introduced by the incomplete data coverage, which makes it necessary to arbitrarily extrapolate the edges of the SAL across data-void areas.

NASA has attempted to overcome these limitations by developing a global assimilation capability of space-based AOD measurements from the Moderate Resolution Imaging Spectroradiometer (MODIS). This new system creates, as part of the atmospheric analysis, a continuous dust distribution which is consistent with aerosol observations, meteorological observations and physical constraints of the atmosphere. In this study, assimilated AOD from MODIS and interactive aerosol modeling are used together in a global framework to investigate the effect of SAL on TC genesis and development.

2. Model and Experiments

This work uses the NASA global data assimilation and forecasting system GEOS-5, developed by the Global Modeling Assimilation Office (GMAO). The GEOS-5 merges a modified version of the National Centers for Environmental Predictions (NCEP) Gridpoint Statistical Interpolation (GSI) analysis algorithm (e.g. Wu et al., [2002]) with the NASA atmospheric global forecast model, as documented in Rienecker et al., [2008]. From the 2008 version, many notable improvements have been applied to the GEOS-5, including the aerosol radiative effects for dust, sea salt, carbonaceous and sulfate aerosols, made possible by the Goddard Chemistry, Aerosol, Radiation and Transport Model (GOCART) module. The GOCART includes aerosol specific processes such as emission, deposition, simplified sulfate chemistry [Colarco et al. 2010], while aerosol advection, diffusion and convection are computed by the host GEOS-5 model. RLD11 used this aerosol modeling capability, but relied on dust concentrations which were dictated by the dust emissions parameterized in the model. While a comparison with observations showed that the aerosol distribution in the initial conditions was realistic, it was nevertheless simulated, and therefore not directly constrained by observations as in a true 'analysis'.

In contrast, this article documents an important advance: the ability to *directly assimilate* AOD derived from MODIS. In near-real time, the GEOS-5 DAS includes assimilation of AOD observations from the MODIS sensorson both the Terra and Aqua satellites. Based on the work of Zhang and Reid [2006] and Lary [2010], a back-propagation neural network has been developed to correct observational biases related to cloud contamination, surface parameterization, and aerosol microphysics, using Aerosol Robotic Network (AERONET) measurements. This empirical algorithm retrieves AOD directly from cloud-cleared MODIS reflectances. On-line quality control is performed with the adaptive buddy check of Dee et al. [2001], with observation and background errors estimated using the maximum likelihood approach of Dee and da Silva [1999]. Following a multi-channel AOD analysis, three-dimensional analysis increments are produced using local displacement ensembles intended to represent misplacements of the aerosol plumes. This new feature allows the GEOS-5 DAS to produce, together with the conventional analysis of meteorological fields, a three-dimensional analysis of dust distribution that is 1) consistent with meteorology at all times and 2) constantly constrained by MODIS observations.

This is an important difference with respect to RLD11, leading to a more accurate representation of the dust distribution and its impact on the atmospheric circulation. It also represents an advance in the field, not yet implemented at this high resolution and in a fully coupled mode in any operational forecasting system.

In this work, a one month-long high-resolution (horizontal: $0.25^o \times 0.3125^o$, vertical: 72 layers) data assimilation is performed with the GEOS-5 DAS, to cover the period from 15 August 2006 to 17 September 2006, corresponding to the well-studied special observing phase (SOP-3) of the NASA African Monsoon Multidisciplinary Analysis (NAMMA) campaign. All conventional and satellite observations used operationally at that time are assimilated, in addition to MODIS-derived AOD. The result is a month of 3-hourly high-quality global meteorological analyses and three-dimensional dust analyses, without data-void areas.

From these analyses, two sets of 31 5-day forecasts at the same resolution are initialized daily at 21 Z, starting from 15 August 2006. The two forecast sets differ by the exclusion (NOA, no aerosol) or inclusion (IAA, interactive aerosol) of the aerosol radiative effects. The length of all the integrations initialized between August 20 and August 28, a period noteworthy for the interaction of intense dust outbreaks with African Easterly Waves (AEWs), is extended to ten days. The increased forecast length allows for a clearer differentiation between the NOA and IAA forecasts (which are both initialized from the same analyses), by allowing for a longer spin-up time. Even if we refer to these 10-day integrations as 'forecasts' we need to clarify that their purpose is to understand physical processes affecting tropical development and not to investigate forecast skill (which is the subject of a future manuscript centered on validation and forecast skill assessment).

3. Results

The impact of interactive aerosols (hereafter Δ_{NOA}^{IAA}) as a function of time t can be defined as a difference $\Delta q(t) = q_{IAA}(t) - q_{NOA}(t)$ of a 3-dimensional meteorological quantity $q(t)$ such as temperature or wind, computed in the IAA and NOA simulations respectively. As noted in RLD11, $\Delta_{NOA}^{IAA}(t)$ is difficult to assess at an instantaneous time because of the intrinsically chaotic nature of the dynamics associated with dust radiative forcing, inhomogeneously distributed and rapidly changing in space and time, and the superposition of the diurnal cycle. In addition, it needs to be clarified that the effect of dust on atmospheric thermal structure is *always* present in the initial conditions, even of the NOA runs. In fact, if dust is present in the real atmosphere at a given time, it is impossible to remove its previous effect on temperature and stability from the initial conditions of an integration. It is only possible to gradually remove the effect of dust from a forecast *after* the initial state, by running an experiment with a NOA configuration for a sufficiently long time. However, even in this case, the impact $\Delta_{NOA}^{IAA}(t)$ increases slowly as a function of integration time. In RLD11, and in this study as well (not shown), a discernible impact can be produced by averaging $\Delta_{NOA}^{IAA}(t)$ through forecast time and across the longitudes of the areas which are affected by high dust concentration. RLD11 main impact was a northward and upward shift of the AEJ, in agreement with other studies (i.e., Wilcox et al. [2010]) and an improvement in regional forecast skill. However, no evident effect on cyclogenesis was found in RLD11.

In contrast, the main result of this work is that after sufficient time from the initial conditions, the dynamical effects of the different radiative forcing imposed by the presence of aerosols start affecting the cyclogenetic process. To this purpose, an example of a clear signal associated with a major dust outbreak is presented. We select the strong outbreak moving from Africa to the Atlantic between 25 and 28 August 2006, which was observed during the NAMMA SOP-3 and discussed in detail by Reale et al. [2009] and Reale and Lau [2010]. These studies did not have aerosol modeling and assimilation capabilities, but investigated the SAL temperature structure (improved by the assimilation of ad-hoc Atmospheric Infrared Sounder (AIRS) temperature profiles) with the aid of the GEOS-5, whose finite-volume dynamics is particularly suitable to maintain fine thermal features and avoid unrealistic dispersion. Their findings suggested the existence of a temperature dipole associated with the dust outbreak: relatively warm at 600-700 hPa and cooler at about 900 hPa or below.

Figure 1 shows the westward progression of the same strong dust outbreak, intercepting the African coastline at about $15^o - 30^o N$, and also the interaction of the dust plume with a broad and weak low pressure area, as represented in the dust analysis produced by the GEOS-5 assimilation between 26 and 27 August 2006.

The complete validation problem is very complex and is beyond the scope of this article, being the subject of a separate study, which will include an assessment of the dust analysis against satellite observations, and the evaluation of the model's forecast skill (with and without aerosol effects) with a variety of metrics. However, a preview of the validation effort is provided. Data from the Cloud-Aerosol Lidar and Infrared Pathfinder Satellite Observations (CALIPSO) and CloudSat, which have allowed a much more accurate understanding of aerosols' optical properties [e.g., Omar et al., 2009] and clouds, are being used for validation. Figures FS1, FS2 and FS3 show comparisons between satellite observations and the corresponding model-generated satellite signals derived from the multi-sensor satellite simulator (documented in Matsui et al. [2013]), which can extract cloud and aerosol profiles from the GEOS-5 as if they were measured from the CALIPSO and CloudSat. The evaluation produced with the satellite simulator shows that the GEOS-5 realistically captured cloud- and mineral dust-affected Lidar backscatter, color ratio, and radar reflectivity in comparison with the observations from CALIPSO and CloudSat sensors (please see supplemental material for a more detailed discussion) over both land and ocean. This preliminary assessment confirms that GEOS5 is able to produce realistic cloud and mineral dust profiles, which is an essential prerequisite for properly simulating the effects of dust on the atmospheric dynamics.

As for the impact on the dynamics, some effects are noted on wind and temperature, when averaged across the forecast time and across longitudes (not shown), as in RLD11. However, since the focus is on TC genesis, the formation of low-level circulations is investigated here in each of the 31 forecasts for both NOA and IAA cases. As a measurement of the TC genesis activity, the minimum value reached by sea-level pressure ($\mathrm{SLP}_{\mathrm{min}}$), and the maximum value reached by 850 hPa relative vorticity (ζ_{max}), as a function of forecast time, are computed over a domain ranging from 5^oN to 20^oN and from 40^oW to 18^oW.

The domain is shown in Fig. 1 and is chosen so as to partly overlap with the eastern side of the so-called Main Development Region. It is slightly more extended to the east (up the African coast) and to the south, where most of the disturbances affected by high dust concentration are noted.

For each individual forecast, a time series of $\mathrm{SLP}_{\min}(t)$ and $\zeta_{max}(t)$ is obtained. At any given forecast time t, the values of $\mathrm{SLP}^{IAA}_{\min}(t)$ and $\zeta^{IAA}_{max}(t)$ (or $\mathrm{SLP}^{NOA}_{\min}(t)$ and $\zeta^{NOA}_{max}(t)$) represent the 'signature' of the most intense low-level circulation created by the model in a IAA (or NOA) configuration within that domain. The impact of the aerosol within the selected domain can thus be assessed by comparing the time series $\mathrm{SLP}^{IAA}_{\min}(t)$ against $\mathrm{SLP}^{NOA}_{\min}(t)$, and $\zeta^{IAA}_{max}(t)$ against $\zeta^{NOA}_{max}(t)$. These do not differ significantly for $t < 120h$, indicating an overall negligible aerosol impact on cyclogenesis during the first 5 days of the forecast (not shown).

As explained before, this is reasonable, because both NOA and IAA sets of forecasts are initialized from the same analysis. Even if the effects of dust are not computed in the NOA integrations, it is impossible to remove them from the initial conditions, because these effects are still present in initial state, whenever dust is present (as in this case). So the NOA and IAA integrations need some spin-up time for the different representation of the physical processes to produce a stronger effect on the dynamics. In order to verify whether the aerosol impact $\Delta^{IAA}_{NOA}(t)$ grows with time and meaningfully affects the cyclogenetic processes, the forecasts initialized between the 20th and the 28th are extended up to ten days. We thus compute the $\mathrm{SLP}_{\min}$ and (ζ_{max}) time series as a function of integration time over the previously referred domain, for each of the 8 IAA

and corresponding NOA ten-day forecasts. The 24-hour running means of all the 8 NOA time series are averaged as function of integration time t, and compared in Fig. 2 to the corresponding IAA ones: the difference $\zeta_{max}^{IAA} - \zeta_{max}^{NOA}$ is statistically significant at 99% beyond day 5. Consistently, the difference $\mathrm{SLP}_{\mathrm{min}}^{IAA}(t) - \mathrm{SLP}_{\mathrm{min}}^{NOA}(t)$ becomes significantly positive, and does not ever change sign at any time t after day 5 (not shown), indicating that if closed circulations form in the NOA environment they tend to have deeper center pressures. In FS4, three individual forecasts, selected among the 8 averaged in Fig. 2, emphasize the different $\Delta_{NOA}^{IAA}(t)$ when strong, moderate or no TC genesis occurs within the domain. If no disturbance forms in the domain throughout a single forecast, or if a disturbance exists but no dust is present, there cannot be an impact on TC genesis: the simultaneous presence of dust and ongoing cyclogenetic processes is necessary for a significant $\Delta_{NOA}^{IAA}(t)$ in an individual forecast.

Figure 3 showcases one of the forecasts and provides a possible mechanism. Both integrations produce a cyclone, but the NOA case is much deeper and lagging behind the IAA. The cyclone is surrounded by dust almost entirely, although the location of the center is in a dust-free area. A zonal vertical cross section at $18^o N$ is taken across the center of the storm in the IAA case and shows the IAA temperature anomaly, obtained by subtracting the mean temperature at the same latitude of a section spanning from $80^o W$ to 20^o in longitude. The warm core of the hurricane (at about $33^o W$) is recognizable, together with the dust-induced temperature dipoles on both sides of it. As in RLD11, a warming is noted in correspondence to the dust level, and a slight cooling below, which increases the static stability at a close distance from the storm, particularly to the west of its center. The last panel of Fig. 3 is obtained by averaging the last 72 hours of the simulation on a zonal section at $22^o N$, so as to intersect the dust plume that is skirting the storm to the north throughout its westward progression. The cross-section illustrates the physical role of dust over the 3 days preceding the snapshot. An evident thermal anomaly is associated with the protruding dust plume towards the ocean, with strong warming at the dust levels, and some cooling on the near-surface levels. The anomalous temperature dipole, which increases the static stability and reduces upward moisture flux in the mid- and low-tropospheric environment surrounding the TC, is the main reason for the overall weaker cyclones in the IAA experiments. Moreover, since the sea-surface temperature is prescribed and the ocean is unable to adjust to the reduction in shortwave radiation, the low-level cooling is probably underestimated.

4. Discussion and concluding remarks

The debate on the possible role of dust on tropical cyclogenesis is complex, due to the inherent difficulties in rigorously proving either argument. Even between studies suggesting a negative SAL effect on TC genesis, there is no overwhelming agreement on whether the intrinsically dryness and high heat content of the SAL dominate the interaction with AEWs, or rather the dust radiative heating. More complexity is added by the treatment of the indirect effects of dust and its microphysical properties [e.g., Van den Heever, 2011; Tao et al. 2012], which however are not discussed in this study.

If we focus on radiative effects only, the debate on their impact often becomes tainted by some degree of subjectivity due to the difficulty of objectively quantifying the SAL and simulating its effect with a realistic distribution of dust. The introduction of assimilated aerosols into a high-resolution global model (already noteworthy for its accurate representation of the tropical atmosphere) allows us to have a better understanding on the aerosol direct radiative effect and its feedback into the dynamics. With these new capabilities we have shown that aerosols radiative effects, computed during a strong dust outbreak, make the environment less conducive to tropical cyclone development. The result is statistically significant and has important implications for medium-range weather forecasting in the tropical Atlantic region.

Acknowledgments. The authors thank Dr. Hal Maring for support through a Calipso-CloudSat grant, and Dr. Tsengdar Lee for allocations on NASA High-End Computing systems. Thanks are due to Mr. Ravi Govindaraju for valuable help with the numerical experiments. The output of the GEOS-5 experiments can be obtained by sending a written request to the corresponding author.

References

Carlson, T. N. and J. M. Prospero, (1972), The large-scale movement of Saharan air outbreaks over the northern equatorial Atlantic, *J. Appl. Meteor., 11* 283-297.

Colarco, P., A. da Silva, M. Chin, and T. Diehl, (2010) Online simulations of global aerosol distributions in the NASA GEOS-4 model and comparison to satellite and ground-based aerosol optical depth. *J. Geophys. Res, 115,* D14207, doi:10.1029/2009JD012820.

Dee, D., and da Silva, A., (1999), Maximum-likelihood estimation of forecast and observation errorcovariance parameters. PartI: Methodology.*Mon. Wea. Rev.,124,* 16691694.

Dee, D., L. Rukhovets, R. Todling, A. da Silva, and J. Larson, (2001), An Adaptive Buddy Check for Observational Quality Control. *Quarterly Journal of the Royal Meteorological Society, 127*, 24512471.

Dunion, J., and C. S. Velden, (2004), The impact of the Saharan Air Layer on Atlantic Tropical Cyclone activity. *Bull. Am. Meteorol. Soc., 85, 353-365.*

Karyampudi, V. M., H. F. Pierce, (2002), Synoptic-Scale Influence of the Saharan Air Layer on Tropical Cyclogenesis over the Eastern Atlantic. *Mon. Wea. Rev., 130,* 31003128.

Lary, D., Remer, L. A., MacNeil, D., Roscoe B., and Paradise, S., (2010), Machine Learning and BiasCorrection of MODIS Aerosol OpticalDepth. *IEEE Geosci. Temote Sens. Lett., 6,* 694.

Matsui, T. T. Iguchi, X. Li, M. Han, W.-K. Tao, W. Petersen, T. LEcuyer, R. Meneghini, W. Olson, C. D. Kummerow, A. Y. Hou, M. R. Schwaller, E. F. Stocker, J. Kwiatkowski (2013), GPM satellite simulator over ground validation sites, Bull. Amer. Meteor. Soc., 94, 16531660.

Omar, A. H., and co-authors, (2009), The CALIPSO automated aerosol classification and Lidar ratio selection algorithm *J. Atmos. Oceanic Technol., 26,* 19942014.

Reale, O., W. K. Lau, K.-M. Kim, E. Brin, (2009), Atlantic tropical cyclogenetic processes during SOP-3 NAMMA in the GEOS-5 global data assimilation and forecast system. *J. Atmosph. Sci., 66,* 3563-3578.

Reale, O., and W. K. Lau, (2010), Reply. *J. Atmosph. Sci., 67,* 24112415.

Reale, O., W. K. Lau, and A. da Silva, (2011), Impact of interactive aerosol on the African Easterly Jet in the NASA GEOS-5 global forecasting system. *Wea. Forecasting, 26,* 504-519.

Rienecker, and co-authors (2008), The GEOS-5 Data Assimilation System. Documentation Versions 5.0.1, 5.1.0 and 5.20 *Technical Report Series on Global Modeling and Data Assimilation,* **27**, NASA/TM-2008-104606, 1-118. Available online at: http://gmao.gsfc.nasa.gov/pubs/tm/

Sun, D., W. K. M. Lau, M. Kafatos, Z. Boybeyi, G. Leptoukh, C. Yang, R. Yang, (2009), Numerical Simulations of the Impacts of the Saharan Air Layer on Atlantic Tropical Cyclone Development. *J. Climate, 22,* 62306250.

Tao, W.-K., J.-P. Chen, Z. Li, C. Wang, and C. Zhang, (2012) Impact of aerosols on convective clouds and precipitation, *Reviews of Geophysics, 50,* RG2001, doi:10.1029/2011RG000369.

Tompkins, A. M., C. Cardinali, J.-J. Morcrette, and M. Rodwell, (2005), Influence of aerosol climatology on forecasts of the African Easterly Jet. *Geophys. Res. Letter., 32*, L10801, doi:10.1029/2004GL022189.

Van den Heever, S. C., G. L. Stephens, and N. B. Wood, (2011), Aerosol indirect effects on tropical convection characteristics under conditions of radiative-convective equilibrium, *J. Atmos. Sci, 68, 699-718.*

Wilcox, E. M., K. M. Lau, and K.-M. Kim, (2010) A northward shift of the north Atlantic Ocean Inter-tropical Convergence Zone in response to summertime Saharan Dust Outbreaks, *Geophys. Res. Lett., 37*, doi:10.1029/2009GL041774.

Wu, W.-S., R.J. Purser and D.F. Parrish, (2002), Three-dimensional variational analysis with spatially inhomogeneous covariances, *Mon. Wea. Rev., 130*, 2905-2916.

Zhang, J., Reid, J. S.(2006), MODIS aerosol product analysis for data assimilation: Assessment of over-ocean level 2 aerosol optical thickness retrievals, *J. Geophys. Res., 111,* D22207, doi:10.1029/2005JD0068.

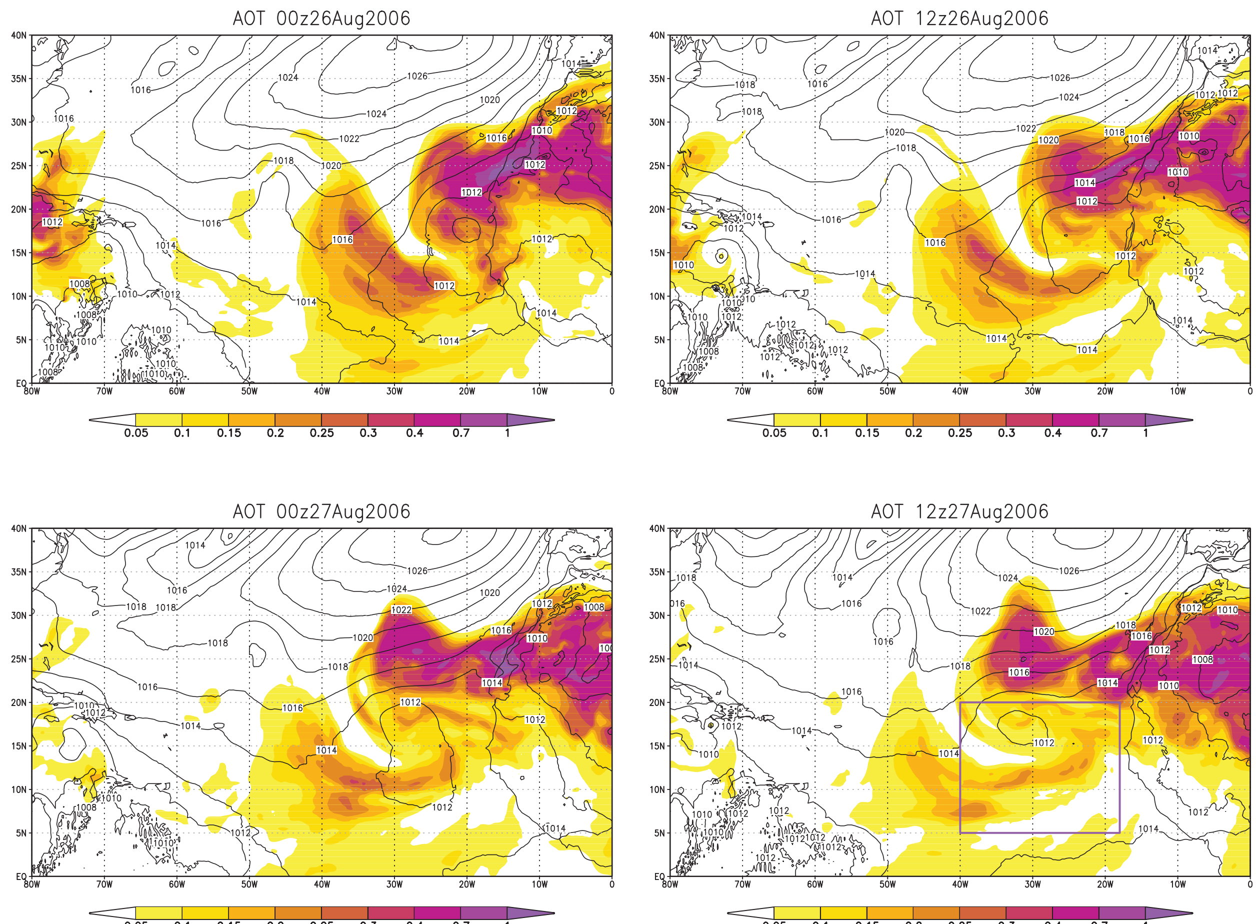

Figure 1. Analysis of Aerosol Optical Depth from the GEOS-5, obtained by assimilation of MODIS optical depth, for 26 August and 27 August 2006.

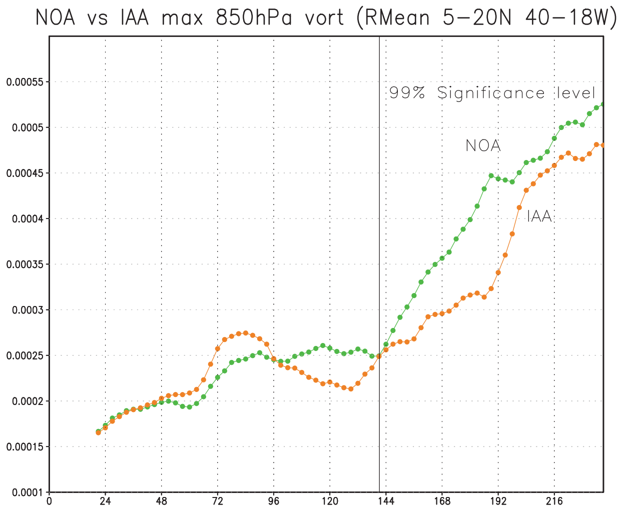

Figure 2. Running 24-hour mean, as a function of forecasting time, for eight NOA and eight IAA forecasts of 850 hPa maximum vorticity. The vorticity maxima are detected at each time step over a chosen domain ($5^oN - 20^oN, 40^oW - 18^oW$), shown in Fig. 1 (lower right panel) which is affected by a strong dust outbreak during the time. The eight forecasts are initialized from 21z19 August to 21z27 August. After day 6, the difference IAA minus NOA is statistically significant at 99%.

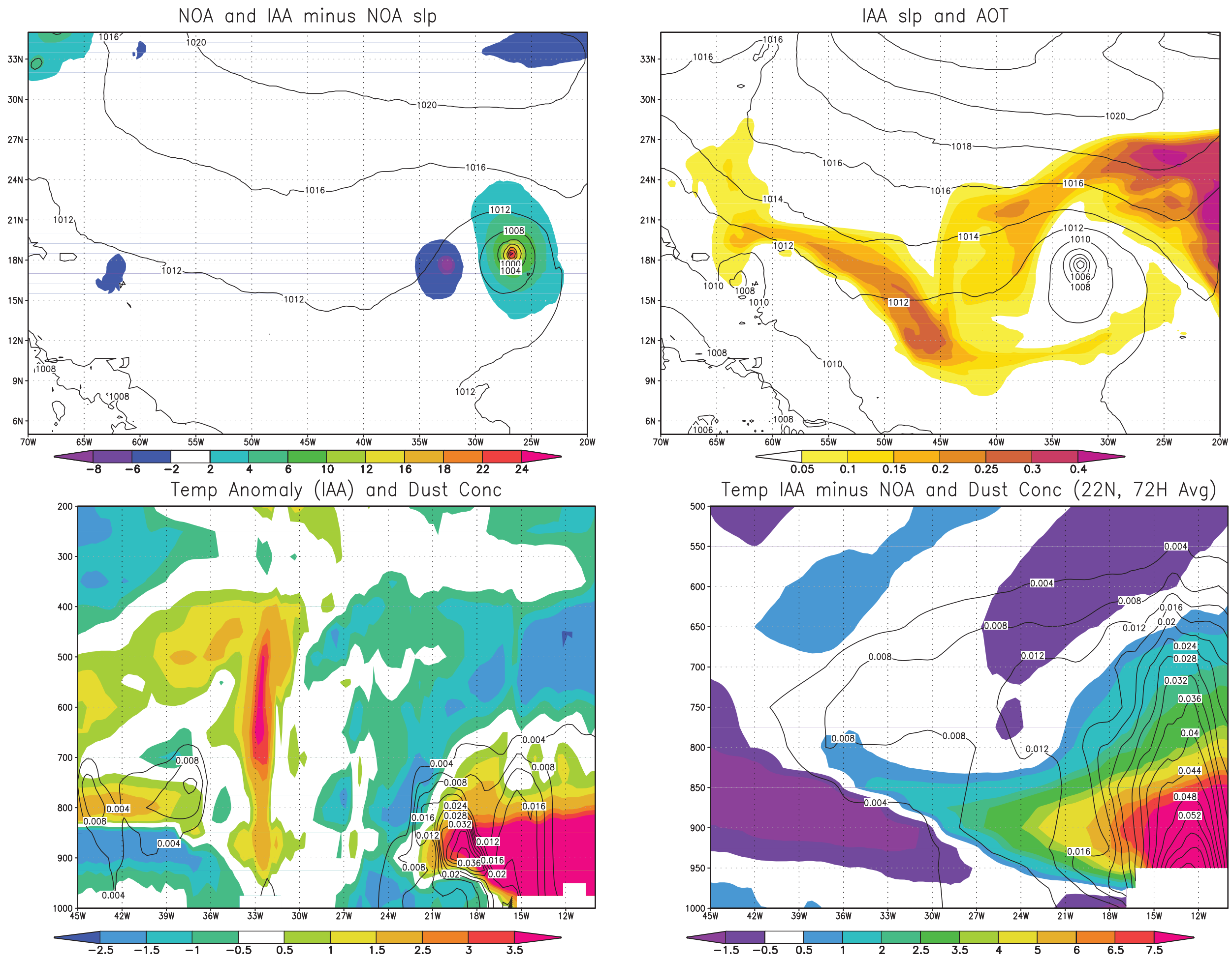

Figure 3. Upper panels: ten day forecast for 18z 2006 5 September, initialized at 21z 26Aug 2006 of NOA slp (hPa, solid) and IAA minus NOA slp departure (shaded, left), and IAA slp (solid) and AOD (shaded, right). Lower left: dust concentration and IAA temperature anomaly (^oC), obtained by subtracting the mean IAA temperature from 60^oW to 20^oW at 18^oN. Lower right: 7 to 10 day forecast, 72 hour average, of IAA minus NOA temperature (shaded) and corresponding mean dust concentration, at 22^oN.